IEICE TRANS. COMMUN., VOL.E94–B, NO.7 JULY 2011

PAPER *Joint Special Section on Opto-electronics and Communications for Future Optical Network*

# Distance-Adaptive Path Allocation in Elastic Optical Path Networks

**Bartlomiej KOZICKI**[†], **Hidehiko TAKARA**[†a)], **Takafumi TANAKA**[†], **Yoshiaki SONE**[†], **Akira HIRANO**[†],
**Kazushige YONENAGA**[†], ***and*** **Masahiko JINNO**[†], ***Members***

**SUMMARY** We describe a concept and realization of distance-adaptive (DA) resource allocation in spectrum-sliced elastic optical path network (SLICE). We modify the modulation format and cross-connection bandwidth of individual fixed-bit rate optical paths to optimize performance with respect to transmission distance. The shorter paths are allocated a smaller amount of resources which allows reducing the spectrum occupied by the channel. We show in calculation a reduction in required spectral resources of more than 60% when compared to the traditional traffic allocation schemes based on ITU-T grid. The concept is verified experimentally.

***key words:*** *all-optical networks, fiber optics links and subsystems, adaptive modulation, quadrature-amplitude modulation, quadrature phase-shift keying*

## 1. Introduction

Optical networks have long been recognized as the most cost-efficient means of transportation for the large volumes of data traffic over metropolitan as well as wide-area networks. In the past, the growing capacity demand stemming from the increasing number of individual users had been satisfied by technological advancements in photonic technologies. The introduction of wavelength-division multiplexing (WDM) and, subsequently, optical erbium-doped fiber amplifiers (EDFAs) had enabled continuous increases in per fiber capacities and, effectively, the allocation of more traffic without significant investments in new fiber plant.

Recent years have seen a development of new data services, such as high-speed broadband access, eScience and grid computing applications as well as ultra-high definition television (UHDTV). With each of those services requiring bandwidths ranging from 10 Gb/s to terabit per second, this growth will rapidly increase the capacity demand on the backbone network supporting the generated traffic. It is expected that in the coming years the overall traffic volume will continue doubling every two years. In such a case, the continuous evolutionary advances in photonic technologies alone may not be able to satisfy the increasing needs in terms of available capacity, space and energy consumption [1].

Two approaches need to be considered simultaneously in order to enable efficient allocation of the demanded traffic. On the one hand is the previously mentioned continuous evolution of photonic technologies. The advances in component bandwidth, multilevel modulation formats as well as amplifier technologies have enabled demonstrations of record-breaking capacity transmission experiments [2]. These advances provide the high capacity optical pipes. On the other hand the need to efficiently support services of varying capacities opens the opportunity for further improvements. Therefore, the second approach to efficient allocation is the adaptation in the optical domain. We have recently proposed novel network architecture based on spectrum-sliced elastic optical paths (SLICE) [3] in which the bandwidth of the optical path and that of the cross-connection changes adaptively depending on the current traffic demand. Other flexible networking schemes including, demonstration of bit rate variable ROADM functionality on an optical orthogonal frequency division multiplexing (OFDM) superchannel [4], format-versatile-transceiver based network model yielding savings on resources compared to single-rate networks [5], routing and spectrum allocation algorithm in an OFDM-based elastic bandwidth optical network [6], and reach optimized architecture for multirate transport system with wavelength-selective switches (WSS) pass-band selection [7], have also been proposed.

In SLICE the adaptation has been experimentally shown to allow scaling of the optical path capacity from 40 to 440 Gb/s. The same architecture was also used to demonstrate aggregation of multiple hundred Gb/s class optical paths into a single continuous super wavelength optical path, enabling efficient allocation of a 1 Tb/s channel in a network consisting of bandwidth-variable wavelength cross connects (BV-WXCs) [8].

In this contribution we focus on distance adaptive (DA) spectrum allocation. Distance adaptive allocation is a novel approach towards adaptation in the optical domain. Its proposal as well as the theoretical investigation of optical signal-to-noise ratio (OSNR) and filtering impairment was presented in our latest paper [9]. In DA-SLICE, the minimum necessary spectral resource is adaptively allocated to an optical path according to end-to-end physical condition of optical path, when the optical path is provisioned in a static fashion. Modulation format and optical filter width are used as parameters to determine the necessary spectral resources to be allocated for an optical path. Here, we extend the study to channel cross-talk and nonlinear penalty evaluation of the distance adaptive scheme. We investigate the feasibility of the scheme for optical paths with an iden-

---

Manuscript received November 9, 2010.
Manuscript revised February 10, 2011.

[†]The authors are with NTT Network Innovation Laboratories, NTT Corporation, Yokosuka-shi, 239-0847 Japan.
a) E-mail: takara.hidehiko@lab.ntt.co.jp

DOI: 10.1587/transcom.E94.B.1823

tical bit rate as a near-term solution in 100 Gb/s systems as well as future super-wavelength optical path systems based on optical OFDM. Distance adaptation in both the WDM approach and the OFDM approach in demonstrated experimentally. Finally, we evaluate the potential to increase the overall spectrum efficiency in future optical transport networks.

## 2. Distance-Adaptive Spectrum Allocation

The distance adaptation for efficient spectrum allocation in optical networks relies on the distribution in lengths of paths in optical networks. An example of three optical paths in a multi-ring network is shown in Fig. 1. Optical path A is an unprotected path, whereas paths B and C are paired route-diverse paths. Depending on the source and destination node, the paths cover different numbers of node hops. Consequently, each of the paths is subjected to a different amount of transmission impairments such as reduction of OSNR, signal filtering, inter-channel cross-talk or nonlinear interaction. In traditional networks, even though the end-to-end penalties differ between different paths, all of the paths are allocated the same spectrum bandwidth and margin for signal degradation. While this ensures that the long-reach paths will be received correctly, it also means that the short-reach paths will have excess power budget at the receiving end. In order to alleviate this inefficiency, we employ DA resource allocation to match the allocated cross-connection bandwidth and signal modulation format to the actual demand for the optical paths. Distance adaptation may be realized in a number of ways. In the following sections we explain the approaches to distance adaptation based on adjustment of:

- cross-connection bandwidth for simple point-to-point links
- modulation format with respect to baud rate for next generation networks employing 100 Gb/s optical channels
- modulation format with respect to the number of carriers for future networks employing super-wavelength optical paths with bit rates of 400 Gb/s.

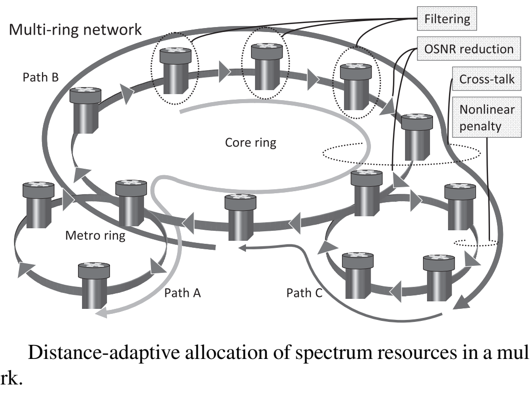

**Fig. 1** Distance-adaptive allocation of spectrum resources in a multi-ring network.

## 3. DA Based on Cross-Connection Bandwidth

The first approach towards optimizing the margin is the DA spectrum allocation considering the cross-connection bandwidth and the resulting filtering effects [10]. In this scheme the amount of allocated spectrum resource depends on the length of the path. The concept is illustrated in Fig. 2. The spectrum is adjusted in units of frequency covering 12.5 GHz. The shorter paths (path on the right-hand side) are allocated 4 units, whereas the longer paths (path on the left-hand side) 5 units. The 3 dB bandwidths of respective channels are 45 GHz and 57 GHz. These values are further reduced after transmission over multiple nodes including respective filters. In both cases the same 112 Gb/s dual polarization (DP) quadrature phase-shift keying (QPSK) modulation is assumed.

The actual distance, expressed in the number of node hops which can be reached with a defined cross-connection bandwidth was investigated in network transmission simulation. The physical model used in the simulation is shown in Fig. 3. In the simulation 112 Gb/s DP-QPSK modulated channels are assumed. The transmitters consist of two optical modulators imprinting QPSK modulation on the optical carriers stemming from the laser diode (LD). The two modulated signals are coupled using a polarization-beam coupler (PBC), thereby producing the X and Y polarization components of DP signal. After amplification in the EDFA, the signal is launched into a 40 km-long transmission span of standard single-mode fiber (SMF) and the corresponding dispersion- compensating fiber (DCF) as well as an optical node model. The BV-WXC node, shown in Fig. 3(b), consists of splitters and bandwidth-variable wavelength-selective switches (BV-WSSes). The filter bandwidth and center frequency can be continuously and seamlessly adjusted to exactly accommodate the optical paths. A 2.5 GHz filter offset is assumed. The transmission fibers and the optical node are placed in a recirculating loop which replicates multi-span transmission over multiple network nodes. The optical signal is received using the coherent receiver which compensated the linear impairments using digital signal processing (DSP). The detailed parameters of the simulation are shown in the table in Fig. 3(c).

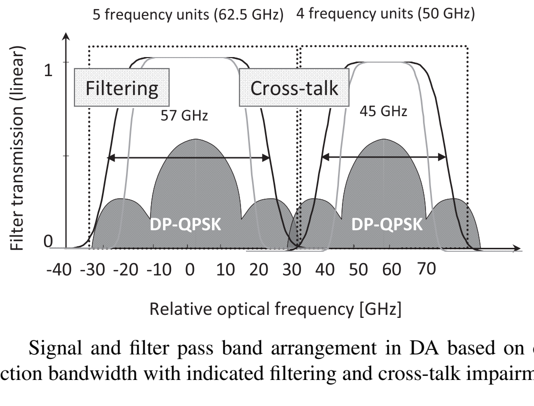

**Fig. 2** Signal and filter pass band arrangement in DA based on cross-connection bandwidth with indicated filtering and cross-talk impairments.

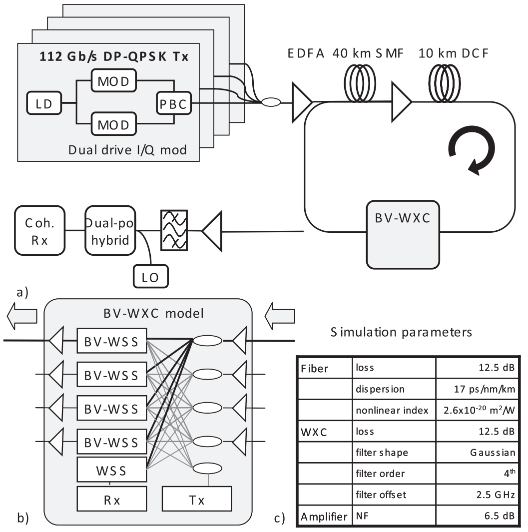

Simulation parameters

| | | |
|---|---|---|
| Fiber | loss | 12.5 dB |
| | dispersion | 17 ps/nm/km |
| | nonlinear index | $2.6\mathrm{x}10^{-20}$ $\mathrm{m}^2/\mathrm{W}$ |
| WXC | loss | 12.5 dB |
| | filter shape | Gaussian |
| | filter order | $4^{\mathrm{th}}$ |
| | filter offset | 2.5 GHz |
| Amplifier | NF | 6.5 dB |

**Fig. 3** Distance-adaptive spectrum allocation based on cross-connection bandwidth adjustment: a) physical model simulation setup; b) BV-WXC architecture; c) simulation parameters.

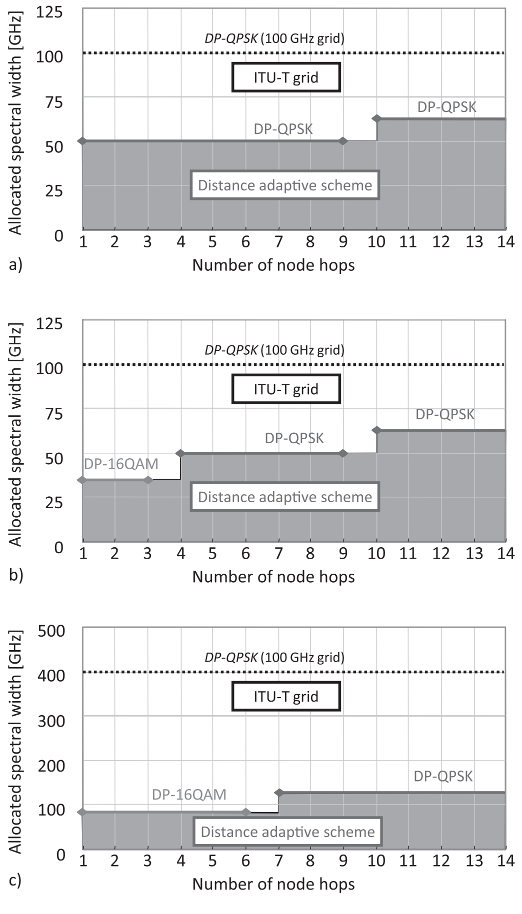

**Fig. 4** DA spectrum resource allocation function for DA schemes based on: a) cross-connection bandwidth adjustment; b) modulation format/baud rate adjustment; c) modulation format/carrier number adjustment with OFDM.

Using the physical model simulation result, we allocate the necessary spectrum resource as a function of node hops. The function is plotted in Fig. 4(a). In the figure, the allocated spectral width is plotted as a function of transmission distance for DA spectrum allocation scheme and compared to the conventional 100 GHz frequency grid scheme. The consumed resource may be understood as contained beneath the solid line for DA spectrum allocation in SLICE and the dotted line for the frequency grid scheme. Increasing the cross-connection bandwidth improves the performance with respect to the number of node hops. Assuming an OSNR margin of 1 dB from the forward error correction (FEC) bit-error ratio (BER) limit of $10^{-3}$, the allocation of 4 frequency units (50 GHz) allows transmission over up to 9 node hops, whereas 5 units are necessary for longer transmission.

## 4. DA Based on Modulation Format and Baud Rate

The second approach to distance-adaptive allocation of traffic optimizes the modulation format in addition to the cross-connection bandwidth used for the given path depending on the amount of impairment experienced by that path [11]. A more robust but less spectrally-efficient modulation is used for the longer paths, whereas, highly-efficient but less robust modulation formats are employed for the shorter paths.

The spectral efficiency of a modulation format may be improved by increasing the density of modulation constellation. For a constant bit rate path, as the number of modulation levels is increased the baud rate is reduced. As a result, WDM channels may be spaced more densely, thereby increasing the amount of data which can be allocated in a given bandwidth. The trade-off in increasing the number of modulation levels lies in the reduced resilience to transmission impairments. As an example in Fig. 5 we consider the relationship between the required signal-to-noise ratio (SNR) and the number of bits per symbol for two families of multilevel modulation formats [12], [13]. The first family represents the phase-only formats and includes bi-

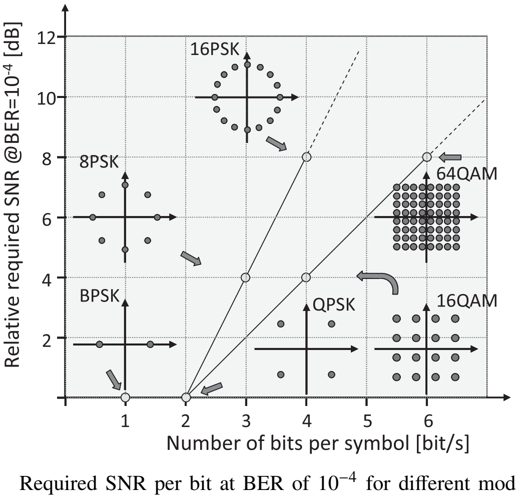

**Fig. 5** Required SNR per bit at BER of $10^{-4}$ for different modulation constellations.

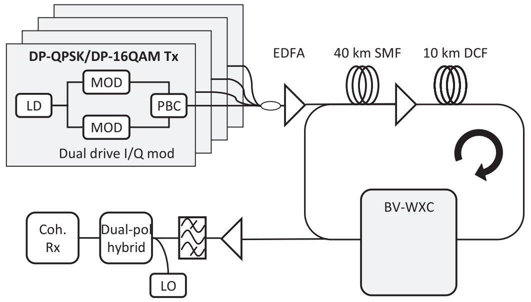

**Fig. 6** Distance-adaptive spectrum allocation based on modulation.

nary phase-shift keying (BPSK), QPSK, and other M-level phase-shift keying formats. The other group involves modulation formats which use both the phase and intensity space and is represented by N-quadrature amplitude modulation formats (NQAM) such as 16QAM and 64QAM. As can be observed in the figure the required SNR increases with the number of modulation levels. The only exception are the DPSK and QPSK formats, which due to the same distance between the points in the constellation have the same required SNR. The figure indicates that for the same number of bits per symbol, the QAM-type modulation formats have lower required SNR than their phase-shift keyed counterparts. The required SNR scales linearly with the OSNR, which in turn is dependent on the number of optical amplifiers traversed in the network. Therefore, by choosing the appropriate modulation format it is possible to optimize the capacity with respect to the desired transmission distance.

The improvement in overall spectrum allocation efficiency achieved by the introduction of DA scheme based on modulation format/baud rate adjustment depends on the choice and performance of the adaptive modulation formats. The selection is guided by the following factors:

- the level of transmission-related impairments
- the number of modulation formats
- the reach of the selected modulation formats.

A physical model simulation was carried out to determine the DA spectrum resource allocation function. The simulation setup is shown in Fig. 6. The simulation parameters are the same as shown in Fig. 3(c). The modulation format of the transmitters can be switched between DP-QPSK and DP-QAM. For all formats a constant bit rate was assumed, which allowed reducing the baud rate of the higher order modulation formats. For the scheme based on modulation format/baud rate adjustment, the distance adaptive spectrum allocation function is plotted in Fig. 4(b). In this case, the 16QAM modulation with 37.5 GHz filter may be used for up to 3 nodes. For optical paths of 4 node hops or more, the QPSK modulation represents the most efficient solution. However, it should be observed that the filter bandwidth of 50 GHz may only be used for paths up to 9 node hops. For longer optical paths, cross-connection bandwidth of 62.5 GHz is necessary. We experimentally demonstrated the concept of distance-adaptive spectrum allocation scheme with modulation format/baud rate adjustment. Multiple WDM optical paths were transmitted over a WXC placed in a recirculating loop mimicking the characteristics of the ring network. The experimental setup is shown in Fig. 7. In this experiment, 16APSK and QPSK formats were used to demonstrate the adaptation. The 16APSK modulation employs 4 phase levels and 4 intensity levels in cross-shaped constellation, which results in constellation point spacing similar to that of 64QAM. As a result, we expect the required OSNR to differ between the two formats by approximately 8 dB according to Fig. 5. We generate 40 Gb/s return-to zero QPSK (RZ-QPSK) signals for the long-reach paths and RZ-16APSK signals for the short reach paths. A multi-carrier source generates 50 GHz-spaced optical wavelength comb aligned to ITU-T frequency grid. The following WSS directs the comb output into one of two modulator branches. One branch contains an RZ modulator and a QPSK modulator driven by data from a pulse pattern generator (PPG). This setup produces 100 GHz-spaced 42.7 Gb/s RZ-QPSK signals. The second branch contains an RZ modulator, a QPSK modulator and a Mach-Zehnder modulator driven by a 4-level electrical signal, producing 10.7 Gbaud, 42.7 Gb/s 16APSK signals. A separate, single 16APSK channel using a narrow linewidth optical source is also generated to test the performance of the multilevel format. All branches are multiplexed in a WSS. 6 QPSK and 10 16APSK signals are transmitted in a recirculating loop containing 40 km of SMF, a DCF, WXC node and a gain equalizing filter. After transmission, both the QPSK and the 16APSK signals are received in an incoherent receiver and analyzed. The QASK and QPSK components after the first node are also shown in Fig. 7.

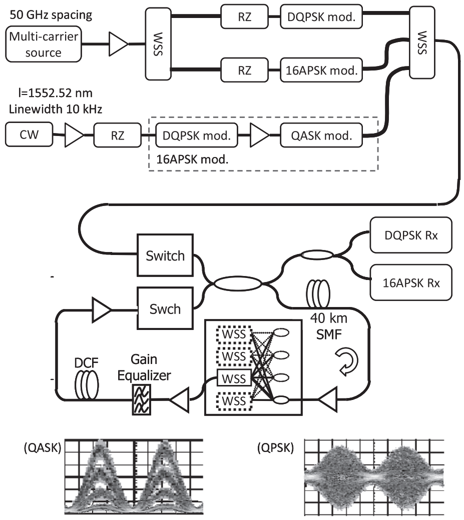

**Fig. 7** Distance adaptive allocation scheme with modulation format/baud rate adjustment- experimental setup.

The performance of the QASK and QPSK components of the 16APSK signal is shown in Fig. 8(a). Both components achieve BER performance better than $10^{-3}$ corresponding to the Q-parameter of 9.8 dB after transmission of up to 5 nodes. It should be noted that the 16APSK mod-

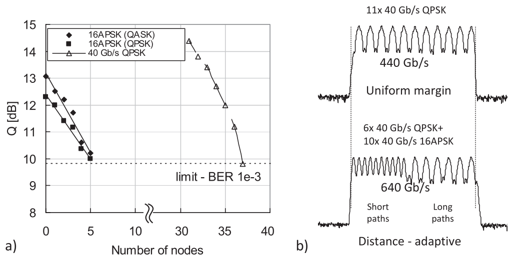

**Fig. 8** Distance-adaptive spectrum allocation experiment results: a) Q performance of QPSK and 16APSK formats; b) optical spectra of transmission with uniform and distance adaptive margin.

ulation depth was adjusted to equalize the performance of the QASK and QPSK components. The 40 Gb/s QPSK signals are influenced by four-wave mixing from the narrowly spaced 16APSK channels (Approx. 0.1 dB penalty per loop) and the accumulation of amplified spontaneous emission (ASE) noise. The Q-factor performance of the QPSK signal is also shown in Fig. 8(a) with the reach of 37 nodes. The difference in achievable transmission distance between the two modulation formats exactly reflects the difference in relative OSNR of 8 dB [14]. The gain in spectrum allocation efficiency achieved in this experiment is illustrated in Fig. 8(b). The traditional approach assuming a uniform margin for all paths modulated by QPSK format is shown in the upper part of the figure. The distance-adaptive case is shown in the lower part of the figure. The distance adaptive spectrum allocation allows transmission of 16 instead of 11 channels, which corresponds to an increase in spectral efficiency of 45%. In other words, a reduction in consumed spectrum resources of 31% could be assumed for transmission of the same amount of traffic.

## 5. DA Based on Modulation Format and Carrier Number

The two distance adaptation schemes discussed so far can be employed in the current optical networks using 100 Gb/s optical channels. In order to efficiently accommodate the traffic in the post 100 Gb/s, future generations of optical networks, we also investigate the DA schemes for super-wavelength optical paths based on optical OFDM. Distance adaptation is realized by employing optical OFDM through the adjustment of the number of subcarriers with respect to the size of modulation constellation [15].

Considering an example of a 400 Gb/s super-wavelength path routing, presented in Fig. 9, in the case of allocation on the ITU-T grid, both a longer path and a shorter path would be allocated the same amount of spectrum resource (Fig. 9(a)). In the DA scheme with optical OFDM, four 100 Gb/s paths are optically aggregated into a single 400 Gb/s super-wavelength optical path with OFDM. For the shorter paths the degree of modulation is increased while the number of subcarriers is decreased. In an example shown in Fig. 9(b) OFDM QPSK (2 bits per symbol, 4 subcarriers) is employed for longer paths, while OFDM 16QAM (4 bits per symbol, 2 subcarriers) is used for the shorter ones. Such approach allows reducing the amount of required spectral resource as the OFDM-based DA scheme realizes much narrower signal spectrum and allows reducing the guard bands when compared to the conventional wavelength-routed optical networks based on the ITU-T grid.

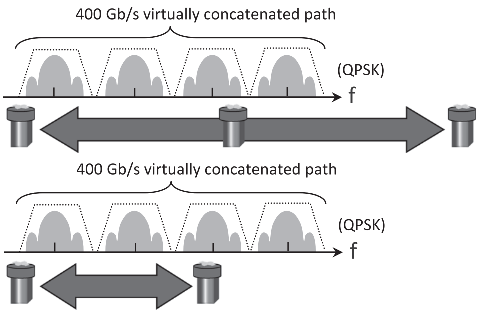

(a) Conventional wavelength-routed optical network

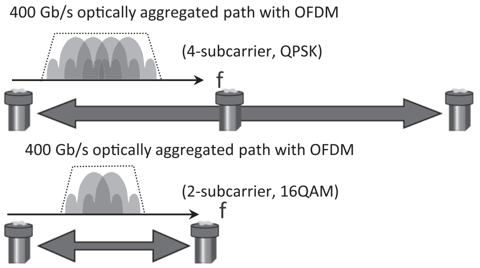

(b) Distance-adaptive SLICE

**Fig. 9** Spectrum allocation for various path distances in DA scheme with adjustment of modulation format/carrier number.

For verification of this DA scheme we used the physical model shown in Fig. 6. For generation of the OFDM signals, the modulator setups with individual modulation patterns were replicated for each carrier with frequency spacing equal to signal baud rate and coupled using an optical coupler. A single 400 Gb/s super-wavelength optical path was considered. QPSK and 16QAM formats were employed. The baud rate of individual carriers was kept fixed, and the constant bit rate was achieved through the adjustment of the number of OFDM carriers: 4 carriers were used for QPSK, and 2 carriers for 16QAM modulation. We performed the simulation including the effects of inter-channel cross-talk as well as nonlinear penalty. In order to investigate the nonlinear performance of the distance adaptive modulation formats, we modified the nonlinear coefficient of the SMF to $2.6\times10^{-20}$ m$^2$/W and set the per channel optical input power to the fiber to 0 dBm.

The distance adaptive spectrum allocation function for the DA scheme based on modulation format/carrier number adjustment is shown in Fig. 4(c). The 400 Gb/s 16QAM-based transmission with cross-connection bandwidth of 87.5 GHz can be realized for up to 6 node hops, whereas the DP-QPSK-based transmission for paths exceeding 7 node hops is required with cross-connection bandwidth of

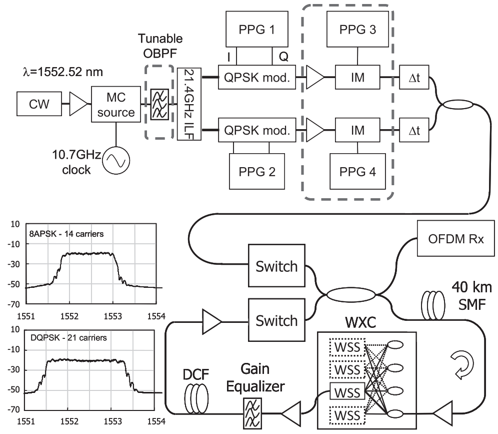

**Fig. 10** Adaptive spectrum allocation — Experimental setup.

137.5 GHz.

The experimental demonstration of the OFDM-based DA scheme is shown in Fig. 10. We use QPSK and 8APSK signals as adaptive modulation formats with 2 bits/symbol and 3 bits/symbol per carrier, respectively. The theoretical difference between the required OSNR of the two formats is 4 dB. Continuous wave (CW) light is modulated by a multi-carrier (MC) source driven by a 10.7 GHz clock to generate uniformly-spaced optical carriers. The number of carriers used for the optical path is adjusted using a tunable optical bandpass filter (OBPF). The spectrum is split into odd and even carriers by a 21.4 GHz interleave filter. The carriers in respective branches are modulated by QPSK modulators and additional intensity modulators (IM) in the case of 8APSK. The odd and even carriers are modulated by different data patterns. The two branches are merged using an optical coupler to form the optical OFDM signal. We generate a 420 Gb/s optical path by using 14 carriers for 8APSK and 21 carriers for QPSK

The adaptation is realized by tuning the OBPF and engaging the IM, as indicated by the dotted line in Fig. 10. The spectra of the respective paths are shown in the insets. The optical paths are transmitted through a recirculating loop reflecting the transmission span and a node in a metro area network. It consists of 40 km of SMF, a WSS-based BV-WXC and a DCF. After the transmission, the performance of the signals is analyzed in the OFDM receiver.

We measured the Q factor (calculated form BER) of one of the center carriers in each path. The results are plotted in Fig. 11 as a function of the number of node hops. Both the QPSK and the ASK components are measured for the OFDM 8APSK optical path. We measure the number of node hops over which the DA signal can be transmitted in the modeled network before the Q factor drops below the FEC limit of 9.8 dB. Both the OFDM QPSK and OFDM 8PSK optical paths suffer an OSNR penalty with the increasing number of node hops. The waveforms of the ASK and QPSK components before the transmission and after 5 node hops are shown in the insets of Fig. 11. As a result, the QPSK signal can be transmitted over 11 nodes, whereas the performance of 8APSK signal exceeds the FEC limit beyond 5 nodes. This reflects the 4 dB difference in required OSNR between the two formats and proves in practice the concept of OFDM-based DA-SLICE.

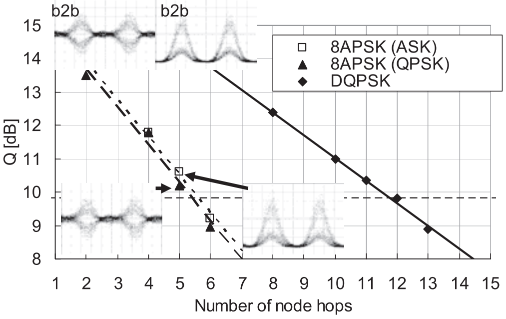

**Fig. 11** Adaptive spectrum allocation — Experimental results.

## 6. Spectrum Allocation Efficiency Improvement

The theoretical and experimental investigation of the DA schemes presented in the previous sections clearly shows the possibility to optimize the margin of optical paths. In order to evaluate the gains in spectrum allocation efficiency brought about by distance adaptation we performed an evaluation using a heuristic routing and spectrum assignment algorithm. The evaluation was carried out by calculating the necessary spectral resources to accommodate a fixed set of connections. A 12-node ring was assumed as the network model. We assess the required total spectrum at the most occupied link in the network.

Our heuristic routing and spectrum assignment algorithm is based on fixed-alternate routing algorithm and first fit algorithm under the spectrum-continuity constraint. An ordered list of a number of fixed routes for each source-destination pair is created based on depth-first search algorithm. For a connection request, a route is selected from the list in sequence. Depending on the number of hops of the route, the number of necessary slots is obtained from the spectrum resource allocation function shown in Fig. 4. The available contiguous frequency slots are searched from a lower-numbered frequency slot to a higher-numbered frequency slot, and then the lowest available contiguous frequency slots are selected. If no available contiguous frequency slots are found on the route, an alternate route is selected from the route list.

In the case of DA scheme based on cross-connection bandwidth adjustment only, the paired route-diverse path has been analyzed. The calculation results are shown in Fig. 12(a). The DA spectrum allocation in SLICE enables a 45% reduction in consumed spectral resources when compared to the fixed frequency grid.

For the DA scheme based on modulation format/baud rate adjustment, the paired route-diverse path case is analyzed. The calculation result is shown in Fig. 12(b). The scheme allows for a 45% reduction in consumed resources compared to the allocation based on ITU-T frequency grid.

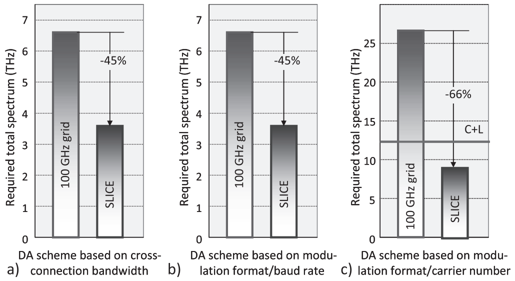

**Fig. 12** Spectrum allocation efficiency simulation results for DA scheme based on: (a) cross-connection bandwidth; (b) modulation format/baud rate; (c) modulation format/carrier number.

Finally, the DA scheme based on modulation format/carrier number adjustment is analyzed in Fig. 12(c). The OFDM-based DA spectrum allocation enables a 66% reduction in consumed spectral resources when compared to the fixed ITU-T grid. The required total spectrum of the fixed ITU-T grid scheme is 26 THz, which cannot be provided by combined C+L bands (12 THz), while that of the DA scheme is reduced to only 8.8 THz. Therefore, the 12 node ring network employing 400 Gb/s class super-wavelength paths could be realized using the DA scheme in SLICE architecture. The actual level of improvement depends on the size and architecture of the network. These results indicate that the DA scheme employing modulation format/carrier number adjustment with OFDM is an attractive way to improve the spectral efficiency for large capacity optical path networks.

## 7. Conclusions

We described the concept and experimental realization of distance-adaptive spectrum allocation scheme. We explained the principle of optimizing the cross-connection bandwidth and modulation format depending on the distance covered by the optical paths, OSNR degradation, filtering penalty, inter-channel cross-talk as well as nonlinear penalty and investigated the properties of DA-SLICE. The adaptive allocation of spectrum resources has been shown to provide savings in consumed spectrum exceeding 60% when compared to the case of traditional ITU-T frequency grid allocation. We demonstrated the concept experimentally and proved its viability in an optical network based on BV-WXCs.

While promising high spectrum efficiency and scalability for future optical transport networks, the SLICE concept presents new challenges on both management and control level and hardware implementation level. Solutions to some of the challenges are presented in our latest reports [16], [17]. We believe that distance adaptation in conjunction with other adaptation techniques will enhance traffic accommodation capability of the existing optical networks as well as the future, post-100 Gb/s systems.

## Acknowledgments

The authors thank Atsushi Watanabe, Masahito Tomizawa, and Osamu Ishida of NTT Network Innovation Laboratories for fruitful discussions.

### References

[1] M. Jinno, H. Takara, and B. Kozicki, "Dynamic optical mesh networks: Drivers challenges and solutions for the future," ECOC 2009, paper 7.7.4, 2009.
[2] A. Sano, H. Masuda, T. Kobayashi, M. Fujiwara, K. Horikoshi, E. Yoshida, Y. Miyamoto, M. Matsui, M. Mizoguchi, H. Yamazaki, Y. Sakamoto, and H. Ishii, "69.1-Tb/s (432×171-Gb/s) C- and extended L-band transmission over 240 km using PDM-16-QAM modulation and digital coherent detection," OFC 2010, paper PDPB7, 2010.
[3] M. Jinno, H. Takara, B. Kozicki, Y. Tsukishima, T. Yoshimatsu, T. Kobayashi, Y. Miyamoto, K. Yonenaga, A. Takada, O. Ishida, and S. Matsuoka, "Demonstration of novel spectrum-efficient elastic optical path network with per-channel variable capacity of 40 Gb/s to over 400 Gb/s," ECOC 2008, paper Th.3.F.6, 2008.
[4] R. Dischler, F. Buchali, and A. Klekamp, "Demonstration of bit rate variable ROADM functionality on an optical OFDM superchannel," OFC 2010, paper OTuM7, 2010.
[5] O. Rival and A. Morea, "Elastic optical networks with 25–100 G format-versatile WDM transmission systems," OECC 2010, paper 7A2–3, 2010.
[6] K. Christodoulopoulos, I. Tomkos, and E. Varvarigos, "Spectrally/bitrate flexible optical network planning," ECOC 2010, paper We.8.D.3, 2010.
[7] A. Gumaste and N. Ghani, "Reach optimized architecture for multi-rate transport system (ROAMTS): One size does not fit all," OFC 2009, paper OMQ3, 2009.
[8] B. Kozicki, H. Takara, Y. Tsukishima, T. Yoshimatsu, T. Kobayashi, K. Yonenaga, and M. Jinno, "1 Tb/s Optical Path Aggregation with Spectrum-Sliced Elastic Optical Path Network SLICE," ECOC 2009, paper 8.3.5, 2009.
[9] M. Jinno, B. Kozicki, H. Takara, A. Watanabe, Y. Sone, T. Tanaka, and A. Hirano, "Distance-adaptive spectrum resource allocation in spectrum-sliced elastic optical path network," IEEE Commun. Mag., vol.48, no.8, pp.138–145, Aug. 2010.
[10] B. Kozicki, T. Tanaka, A. Watanabe, Y. Sone, T. Tanaka, A. Hirano, K. Yonenaga, and M. Jinno, "Distance-adaptive spectrum allocation in SLICE considering optical filtering effects," OECC 2010, paper 7A2-2, 2010.
[11] B. Kozicki, H. Takara, Y. Sone, A. Watanabe, and M. Jinno, "Distance-adaptive spectrum allocation in elastic optical path network (SLICE) with bit per symbol adjustment," OFC 2010, paper OMU3, San Diego, 2010.
[12] K-P. Ho, Phase-modulated optical communication systems, Chap. 9, Springer, 2005.
[13] R.J. Essiambre, G. Kramer, P.J. Winzer, G.J. Foschini, and B. Goebel, "Capacity limits of optical fiber networks," J. Lightwave Technol., vol.28, no.4, pp.662–701, Feb. 2010.
[14] D.C. Kilper and W. Weingartner, "Monitoring optical network performance degradation due to amplifier noise," J. Lightwave Technol., vol.21, no.5, pp.1171–1178, May 2003.
[15] H. Takara, B. Kozicki, Y. Sone, T. Tanaka, A. Watanabe, A. Hirano, K. Yonenaga, and M. Jinno, "Distance-adaptive super-wavelength routing in elastic optical path network (SLICE) with optical OFDM," ECOC 2010, paper We.8.D.2, 2010.
[16] M. Jinno, Y. Sone, and A. Hirano, "Management and control aspects of spectrum-sliced elastic optical path network," ECOC 2010 Workshop, 2010.
[17] B. Kozicki, H. Takara, Y. Tsukishima, T. Yoshimatsu, T. Kobayashi,

K. Yonenaga, and M. Jinno, "Experimental demonstration of spectrum-sliced elastic optical path network (SLICE)," Opt. Express, vol.18, no.21, pp.22105–22118, 2010.

**Bartlomiej Kozicki** received the M.Sc. degree from the Technical University of Lodz, Poland, and the Ph.D. degree in telecommunications engineering from Osaka University, Japan. Since 2008, he has been with NTT Network Innovation Laboratories, Japan. His research interests include large capacity optical transmission systems, advanced modulation formats and optical measurement techniques. Dr. Kozicki received the IEEE/LEOS Student Award in 2007. He is a member of the IEEE.

**Hidehiko Takara** received the B.S., M.E., and Ph.D. degrees in electrical engineering from the University of Keio, Kanagawa, Japan, in 1986, 1988, and 1997, respectively. In 1988, he joined Nippon Telegraph and Telephone Corporation (NTT) Transmission Systems Laboratories, Kanagawa, Japan. Currently, he is a Senior Research Engineer in NTT Network Innovation Laboratories, NTT Corporation. His research interests include ultrahigh-speed and large capacity optical transmission systems and optical measurement techniques.

**Takafumi Tanaka** received his B.E. degree in electrical engineering and M.S. degree in informatics from the University of Tokyo, Japan, in 2007 and 2009, respectively. In 2009 he joined NTT Network Innovation Laboratories. His main research interests are photonic network architecture and its control technology.

**Yoshiaki Sone** received his B.E. and M.E. degrees in electronics engineering from Tohoku University, Sendai, Japan, in 2001 and 2003, respectively. In 2003, he joined the NTT Network Innovation Laboratories and has been engaged in research on control technology of photonic transport networks. His research interest lies in network architecture, resilience schemes, design of protocols for distributed control such as ASON/GMPLS, and interoperability testing of such protocols.

**Akira Hirano** received the B.S. degree in physical chemistry and the M.S. degree in astrophysics from Osaka University, Osaka, Japan, in 1990 and 1993, respectively. In 1993, he joined the NTT Corporation, Kanagawa, Japan, and is currently with the NTT Network Innovation Laboratories, where he is involved in the lightwave communications area. His main interests are in the high-speed lightwave transport systems, optical signal processing, and ultra short pulse generation.

**Kazushige Yonenaga** received the B.E. and M.E. degrees in electrical engineering from Keio University, Yokohama, Japan, in 1989 and 1991, respectively. In 1991, he joined the Nippon Telephone and Telegraph (NTT) Transmission Systems Laboratories, Yokosuka, Japan, where he has been engaged in research on coherent optical communication and high-speed WDM transmission systems. From 2000 to 2004, he was with NTT Electronics Corporation. He is currently with NTT Network Innovation Laboratories. His current research interests include optical transparent networks and its enabling technologies.

**Masahiko Jinno** is a Senior Research Engineer, Supervisor, in NTT Network Innovation Laboratories. He received the B.E. and M.E. degrees in electronics engineering from Kanazawa University, Ishikawa, and the Ph.D. degree in engineering from Osaka University, in 1984, 1986, and 1995, respectively. He joined NTT in 1986. He was a guest scientist at the National Institute of Standards and Technology (NIST), Boulder, Colorado, USA, during 1993–1994. He received the Young Engineer Award from the Institute of Electronics, Information and Communication Engineers (IEICE) in 1993, the Best Paper Awards for the 1997, 1998, and 2007 Optoelectronics and Communications Conferences (OECC), and the Best Paper Award for the 2010 ITU-T Kaleidoscope Academic Conference.